PCP
PLANT & CELL PHYSIOLOGY

RD20, a Stress-Inducible Caleosin, Participates in Stomatal Control, Transpiration and Drought Tolerance in *Arabidopsis thaliana*

Yann Aubert[1], Denis Vile[2], Marjorie Pervent[2], Didier Aldon[1], Benoit Ranty[1], Thierry Simonneau[2], Alain Vavasseur[3] and Jean-Philippe Galaud[1,*]

[1]Université de Toulouse, UPS, UMR CNRS 5546, Surfaces Cellulaires et Signalisation chez les Végétaux, BP 42617, 31326 Castanet-Tolosan, France

[2]INRA, SUPAGRO, UMR759 Laboratoire d'Ecophysiologie des Plantes sous Stress Environnementaux (LEPSE), 2 place Pierre Viala, 34060 Montpellier Cedex, France

[3]Laboratoires des Echanges Membranaires et Signalisation; UMR 6191, CNRS-CEA-Université Aix-Marseille II, Commissariat à l'Energie Atomique-Cadarache Bat 156, 13108 Saint-Paul-lez-Durance, France

*Corresponding author: E-mail, galaud@scsv.ups-tlse.fr; Fax, +33-534-32-38 02

(Received July 27, 2010; Accepted October 8, 2010)

Plants overcome water deficit conditions by combining molecular, biochemical and morphological changes. At the molecular level, many stress-responsive genes have been isolated, but knowledge of their physiological functions remains fragmentary. Here, we report data for *RD20*, a stress-inducible Arabidopsis gene that belongs to the caleosin family. As for other caleosins, we showed that RD20 localized to oil bodies. Although caleosins are thought to play a role in the degradation of lipids during seed germination, induction of *RD20* by dehydration, salt stress and ABA suggests that RD20 might be involved in processes other than germination. Using plants carrying the *promoter RD20::uidA* construct, we show that *RD20* is expressed in leaves, guard cells and flowers, but not in root or in mature seeds. Water deficit triggers a transient increase in *RD20* expression in leaves that appeared predominantly dependent on ABA signaling. To assess the biological significance of these data, a functional analysis using *rd20* knock-out and overexpressing complemented lines cultivated either in standard or in water deficit conditions was performed. The *rd20* knock-out plants present a higher transpiration rate that correlates with enhanced stomatal opening and a reduced tolerance to drought as compared with the wild type. These results support a role for RD20 in drought tolerance through stomatal control under water deficit conditions.

Keywords: *Arabidopsis thaliana* • Caleosin • Drought tolerance • Oil bodies • Stomata.

Abbreviations: AtCLO, *Arabidopsis thaliana* caleosin; BAC, bacterial artificial chromosome; CaMV, cauliflower mosaic virus; ER, expansion rate; GFP, green fluorescent protein; GUS, β-glucuronidase; KO, knock-out; OB, oil body; RD20, Responsive to Dehydration 20; RT–PCR, reverse transcription–PCR; RWC, relative water content; WT, wild type; WUE, water use efficiency.

Introduction

Plant growth is greatly altered by abiotic stresses such as drought, salt stress or cold. In order to survive and propagate in fluctuating environments, plants have developed a variety of tolerance mechanisms including the protection of membranes and the production of osmolytes to maintain water and ion homeostasis (Bartels and Sunkar 2005). At the onset of water deficit, one of the most rapid responses observed is the closure of stomata, followed, on a longer time scale, by reduced plant growth decreasing transpiration and facilitating the conservation of water (Westgate and Boyer 1985). To activate these responses, genetic reprogramming is required, and several hundred genes have been identified as stress responsive (Kreps et al. 2002, Oono et al. 2003, Kant et al. 2008). The up-regulated genes can be classified as early and transiently induced genes that encode proteins involved in signaling and gene regulation, and late induced genes whose products are mainly involved in cell protection (Bray 2004). Among the early induced genes, *RD20* (Responsive to Dehydration, 20) appears to be one of the most highly expressed and is now often used as a stress marker gene (Magnan et al. 2008, Alexandre et al. 2009), although its actual role in stress responses remains unknown. The protein encoded by *RD20* is 236 amino acids long and belongs to the caleosin family. This family is composed of at least seven members in Arabidopsis (AtCLO1, 2, 3/RD20, 4.1, 4.2, 5.1 and 5.2) and RD20 exhibits about 65% amino acid identity with

Plant Cell Physiol. 51(12): 1975–1987 (2010) doi:10.1093/pcp/pcq155, available online at www.pcp.oxfordjournals.org

AtCLO1/AtCLO2, and 45% with AtCLO4.1 and 4.2/AtCLO5.1 and 5.2 (Partridge and Murphy 2009). Caleosins share a unique functional calcium-binding domain in the N-terminal region (Takahashi et al. 2000), a central hydrophobic domain and a proline knot motif presumably responsible for protein targeting to oil bodies (OBs) (Abell et al. 1997, Chen and Tzen 2001). The first identified caleosin was isolated in rice and named OsEFA27 for EF-hand Anchored 27 kDa protein. Interestingly, *OsEFA27* was isolated in a cDNA library obtained from ABA-treated germinating rice seedlings, and the authors reported that *OsEFA27* mRNA also accumulated in vegetative tissues in response to dehydration and NaCl (Frandsen et al. 1996). In Arabidopsis, caleosin gene expression patterns revealed that *AtCLO1* and *AtCLO2* are mainly expressed during seed maturation and during the first days following germination (Naested et al. 2000). *AtCLO4.1*, *5.1* and *5.2* mRNA expression levels are low but detectable in root, leaf, shoot and flower tissues, and, as for other caleosins, they are not induced in response to dehydration or ABA treatment (Hruz et al. 2008). Thus, *RD20* gene expression is rather different because of its induction by various abiotic factors (Kant et al. 2008). As yet, little is known about the physiological function of caleosins and few functional analyses have been performed. Poxleitner et al. (2006) showed that loss of function of AtCLO1 is responsible for a defect in post-germinative growth and that *atclo1* knock-out (KO) mutants grew more slowly than the wild type (WT) and showed a higher number of OBs and vacuoles per cell. Subcellular localization of AtCLO1 in developing rapeseed embryo revealed that AtCLO1 is associated with microsomal and OB fractions (Naested et al. 2000) and, more recently, Hanano et al. (2006) demonstrated that AtCLO1 (referred to as AtPXG1), AtCLO2 (AtPXG2) and OsEFA27 possess a Ca^{2+}-dependent peroxygenase activity. The recombinant proteins catalyze co-oxidation reactions typical of peroxygenase activity in microsomes and lipid droplet fractions. AtCLO1 contains a heme responsible for its enzymatic activity, and the highly conserved His70 and His138 are essential to the peroxygenase activity and to the heme coordination. All these data suggest that some caleosins are involved in mobilization or degradation of OBs and storage lipids during embryo development and germination, but they raise the question of the role of the other caleosin isoforms and particularly of RD20 in Arabidopsis stress responses.

In this work, functional genomics and ecophysiological approaches were coupled to evaluate the role of RD20 in response to abiotic stresses and ABA in Arabidopsis. The subcellular localization of RD20 was investigated, the spatio-temporal expression pattern of *RD20* was determined using a *promoter RD20::GUS* (*pRD20::GUS*) reporter construct, and functional analyses of *rd20* KO and KO complemented transgenic lines were performed. The transpiration rate and detailed parameters of plant growth were analyzed in modified lines under controlled and water deficit conditions using the automated platform PHENOPSIS (Granier et al. 2006). Finally, measurements of stomatal aperture and drought tolerance assays were performed.

Results

RD20 is an OB-associated protein

RD20/AtClO3 protein belongs to a small multigenic family in Arabidopsis (Partridge and Murphy 2009), and several works showed that some caleosins are OB-associated proteins (Frandsen et al. 1996, Naested et al. 2000, Murphy et al. 2001). Caleosins, as the oleosins that are considered as the major proteins found in plant OBs, share a central hydrophobic domain with a proline knot motif presumably responsible for their targeting to OBs (Abell et al. 1997, Chen and Tzen 2001). To analyze the subcellular localization of RD20, an RD20–green fluorescent protein (GFP)–β-glucuronidase (GUS) fusion protein was transiently expressed under the control of the cauliflower mosaic virus (CaMV) 35S constitutive promoter in onion epidermal cells (**Fig. 1**). Fluorescence of GFP is observed in spherical-shaped mobile structures, suggesting that RD20 is associated with OBs (**Fig. 1E, F**; **Supplementary video online**). To confirm the nature of these GFP-labeled structures, Nile red, a neutral lipid dye regularly used as an OB marker (Greenspan et al. 1985, Schimdt and Herman, 2008), was used to visualize OBs in onions transformed cells by fluorescence imaging (**Fig. 1G, H**). A merge of the images shown in **Fig. 1E and G** shows that GFP and Nile red fluorescences co-localize, and this supports RD20 being associated with OBs (**Fig. 1I**). As a control, a GFP–GUS fusion protein was transiently expressed under the CaMV 35S constitutive promoter and fluorescence imaging showed that the corresponding protein is present in the cytosol as well as in the nuclear compartment (**Fig. 1A–C**). Collectively, these data indicate that RD20, as demonstrated for AtCLO1 and AtCLO2, is an OB-associated protein.

RD20 is differentially expressed during Arabidopsis development

Thanks to increasing microarray analyses, abundant information is now available concerning Arabidopsis gene expression. Here, to gain new insights into *RD20* gene expression patterns, we investigated the temporal and spatial gene regulation of *RD20*. Transgenic plants carrying a 1.5 kb region upstream of the start codon of the *RD20* gene fused to the GUS reporter gene were obtained. To rule out the presence of putative regulatory elements in the *RD20* coding region including introns and exons as shown by Schauer et al. (2009) for the *AGAMOUS-LIKE6* gene, transgenic plants have also been generated with a construct carrying the *RD20* promoter region and the entire coding region fused to the GUS reporter gene. GUS staining was performed on three independent lines carrying each construct, and the results showed that all lines presented the same GUS staining pattern, indicating that no major regulatory elements are present in the coding regions of *RD20*. The results presented here are only those obtained with *pRD20::GUS* transgenic plants (**Fig. 2**). GUS activity was detected only in above-ground tissues whatever the developmental stage. This is consistent with available data in several microarray databases (Hruz et al. 2008).

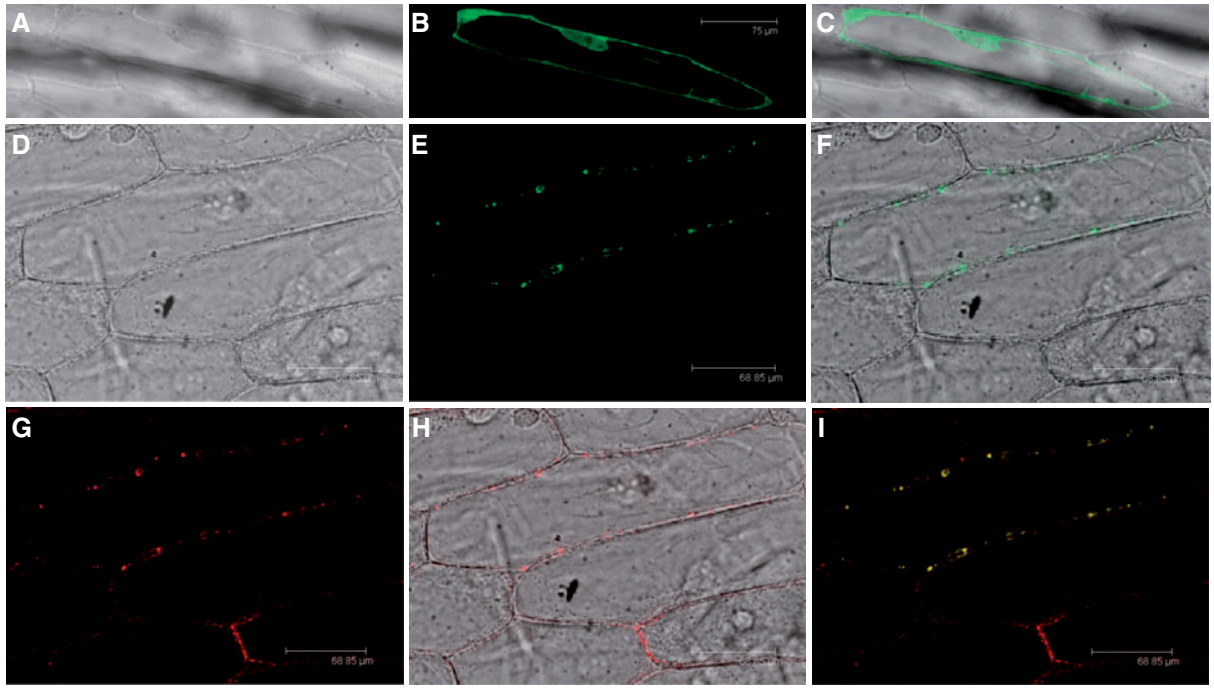

Fig. 1 Subcellular localization of an RD20–GFP–GUS fusion protein in onion epidermal cells. Confocal imaging of a control GFP–GUS fusion protein: (A) bright field image, (B) GFP fuorescence, (C) merge of A and B. Confocal imaging of the RD20–GFP–GUS fusion protein: (D) bright field image, (E) GFP fluorescence, (F) merge of D and E. (G) Confocal imaging of Nile red fluorescence: (H) merge of D and (G); (I) merge of E and G.

In standard culture conditions, GUS activity was low and, to obtain a visible signal, incubations in staining solution were performed for 6–24 h. In young (3- to 5-day-old) seedlings, GUS activity was detected in the cotyledons and hypocotyl (**Fig. 2C, D**); in 20-day-old seedlings, a low but detectable expression was observed in leaves (**Fig. 2E**) and at a higher magnification a signal was observed in specialized structures such as hydatode and trichome bases (**Fig. 2F**; open and filled arrow, respectively). Staining of leaf epidermal peels revealed a stronger GUS activity in guard cells and neighboring cells compared with other epidermal cells (**Fig. 2G**). At the reproductive stage, GUS activity was detected in limited zones of the flower (**Fig. 2H, I**), including the stigmatic papillae, stamens and sepals. Finally, histochemical staining of siliques revealed that GUS activity was detected in the first days following fertilization (green silique) (**Fig. 2J**) but was detectable neither in mature brown siliques (**Fig. 2K**) nor in mature dry seeds (**Fig. 2A, B**). Therefore, this analysis indicates that although *RD20* is expressed at a low level throughout plant development, its expression pattern is limited to above-ground organs and some specialized leaf tissues.

RD20 expression is responsive to various abiotic stimuli and ABA

It has been reported that *RD20* expression is enhanced by ABA, salt, dehydration and osmotic stresses by using microarray approaches or Northern blot experiments (Takahashi et al. 2000, Seki et al. 2001). We confirmed these data by quantitative reverse transcription–PCR (RT–PCR) by measuring *RD20* transcripts levels and *RAB18*, a well-known stress- and ABA-responsive gene, as a control (Lang and Palva 1992). Data obtained indicated that dehydration and ABA induced a rapid and transient increase of *RD20* gene expression, with a 150-fold increase 2 h after dehydration and up to 300-fold 3 h after ABA treatment (**Fig. 3A, B**). The importance of ABA signaling in *RD20* gene expression was then assessed by comparing the responses of *RD20* gene expression to dehydration in WT and ABA-deficient (*aba1-5*) or ABA-insensitive (*abi1-1*) mutants (**Fig. 3C**). *RD20* gene expression was dramatically reduced in those mutants, indicating that following dehydration, *RD20* gene expression is mostly an ABA-dependent process. Then we took advantage of the *pRD20::GUS* transgenic lines to evaluate the spatio-temporal pattern of *RD20* gene expression in response to environmental changes. Transgenic plants were cultivated on Murashige and Skoog (MS) medium and subsequently transferred on NaCl- or mannitol-supplemented MS medium for different times or detached leaves were submitted to a dehydration treatment for 2 h prior to GUS staining. As expected, GUS staining was stronger and observed more rapidly following these treatments compared with plants cultivated in control conditions. No difference in the spatial expression patterns were observed between stress-treated and control plants, indicating that its induction by stress conditions only occurred in cells having a basal level of *RD20* gene expression (**Supplementary Fig. S1**). *RD20* gene expression was also analyzed following mechanical stress. Dark blue staining

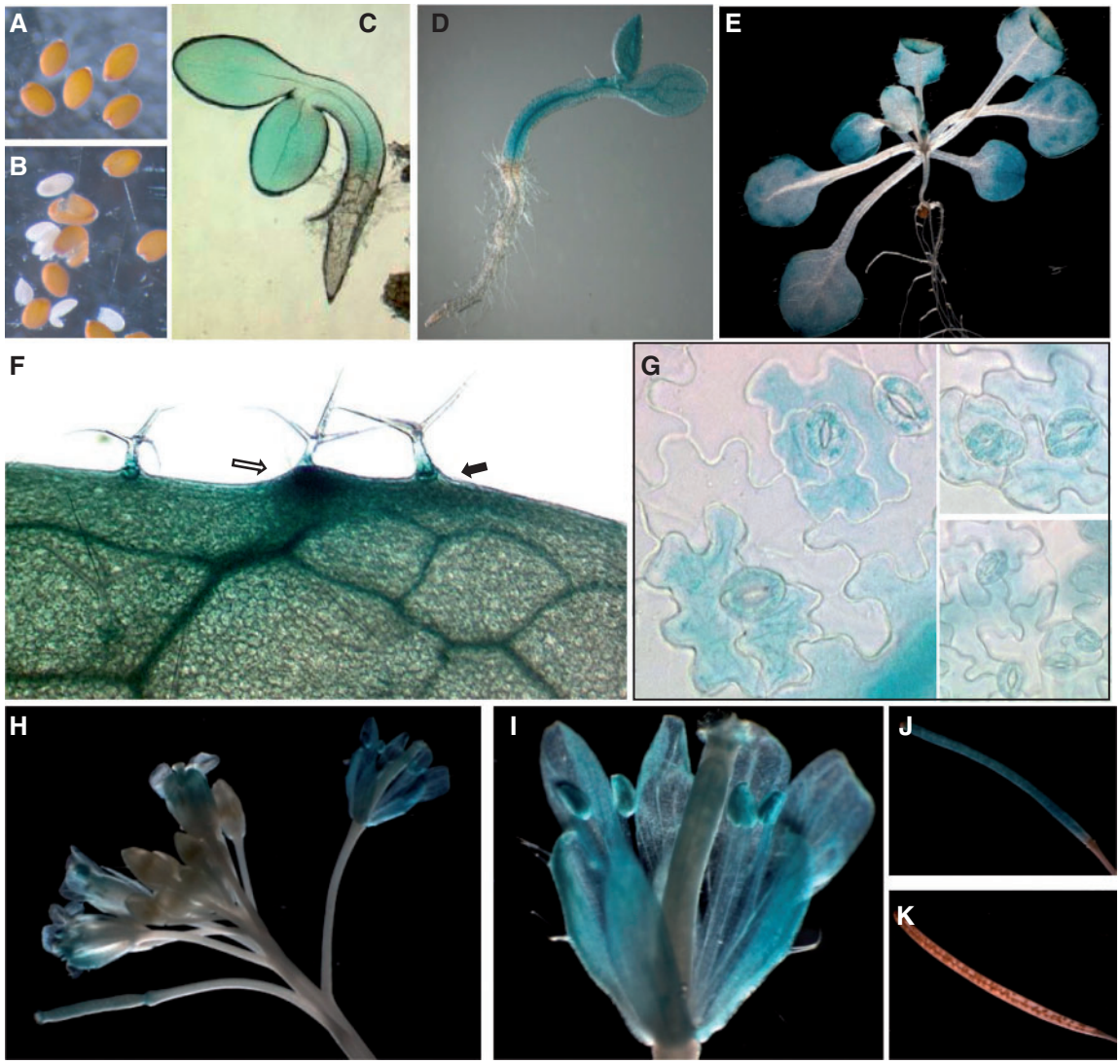

Fig. 2 Expression patterns of the *RD20* gene. Histochemical GUS staining of transgenic plants transformed with a 1.5 kb *promoter RD20::GUS* reporter (*pRD20::GUS*). T_3 generation plants were stained with X-Gluc for 6–24 h. The observations illustrated are representative of the patterns obtained with three independent transgenic lines. (A) Dry mature seeds; (B) dry mature seeds without the tegument; (C) 3-day-old seedling; (D) 5-day-old seedling; (E) 20-day-old seedling; (F) detail of a 35-day-old leaf showing GUS expression at the base of the trichomes (filled arrow) and in a hydatode (open arrow); (G) epidermal peels of 35-day-old leaves showing GUS coloration in guard cells and neighboring cells in three independent T_3 pRD20:GUS transgenic lines; (H) inflorescence from a 45-day-old *pRD20::GUS* plant showing GUS expression in flowers and siliques; (I) magnification of the flower presented in H showing GUS expression in the stigmatic papilla, petals, sepals and stamens (mainly in the anthers). (J) Young green silique and (K) mature brown silique.

restricted to holes made with a needle indicated that *RD20* transcription is induced 2 h after leaf wounding (**Supplementary Fig. S1**). Overall, these data indicate that *RD20* is expressed in many organs and tissues during development, morphogenesis and in response to ABA and abiotic stresses.

Analysis of transgenic lines modified in *RD20* gene expression

To examine the function of RD20, a reverse genetic approach was developed using a T-DNA insertional mutant in the Ws-4 accession. Homozygous mutant lines were obtained, and PCR experiments on genomic DNA as well as sequence analyses confirmed the T-DNA insertion site in the second exon of the *RD20* gene (**Fig. 4A**). This insertion results in the lack of a full-length *RD20* transcript (**Fig. 4B**, *F1-R3*), but detection of a chimeric *T-DNA-RD20* transcript raises the possibility that this mutation leads to a dominant-negative phenotype (**Fig. 4B**, *F1-R2*). The KO mutant was complemented with a *Promoter 35S::RD20* construct (named ORK for overexpression of *RD20* in KO *rd20*) to generate ORK5-complemented transgenic plants. Southern blot analysis using T-DNA as a probe indicated that ORK5 contains at least two insertional copies of the transgene.

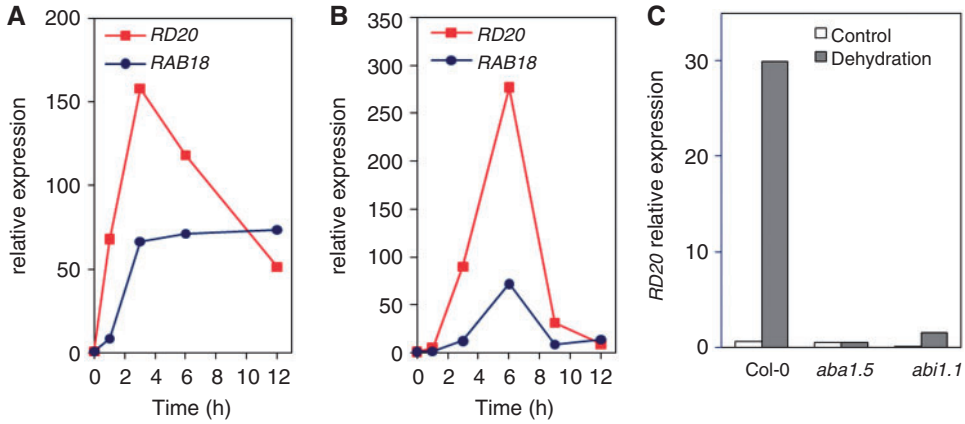

Fig. 3 Real-time RT–PCR analyses of *RD20* gene expression in *Arabidopsis thaliana* plants subjected to abiotic stimuli. (A, B) Total RNA from 10-day-old WT seedlings or leaves was analyzed by quantitative RT–PCR with gene-specific primers for *RD20* and for a stress- and ABA-responsive gene, *RAB18*. The transcript levels of *RD20* and *RAB18* are plotted as the relative expression (fold) of plants exposed to dehydration (A) for the indicated period of time or (B) to ABA (100 μM). Transcript levels of *β-tubulin* were used for standardization. (C) Quantitative RT–PCR analyses of *RD20* gene expression in the WT, the ABA-deficient mutant *aba1-5* and the ABA-insensitive mutant *abi1-1* subjected to dehydration for 120 min. Total RNA was prepared from 4-week-old rosettes. *Desmin*, an external mRNA, was used as a control for data standardization. The results presented correspond to a representative experiment of two biological and three technical replicates.

Expression of the transgene was analyzed in ORK5 and a 5-fold increase in *RD20* transcript level was observed compared with wild-type plants (**Fig. 4C**). The presence in the Arabidopsis genome of several transcribed caleosin genes raises the possibility that other caleosins could compensate for the loss of *RD20* transcripts in the *rd20* mutant. Thus, semi-quantitative RT–PCRs were performed to check if the expression profiles of others caleosins were modified in the *rd20* mutant, as well as in the ORK5-complemented transgenic line. As expected, constitutive expression of *RD20* was observed in the ORK5-complemented line and was absent in the *rd20* mutant (**Fig. 4D**); concerning the expression of other caleosin genes, no modifications were observed in those lines compared with the WT (**Fig. 4D**). This experiment was also performed using plants submitted to water deficit conditions. In this case, *RD20* mRNA content increased following dehydration treatment in the WT, whereas mRNAs level of other caleosins did not present variations in WT, *rd20* and ORK5 lines (not shown). Overall, these data indicate that among caleosins, RD20/AtCLO3 plays a specific role in Arabidopsis response to abiotic stresses compared with other caleosins present in the Arabidopsis genome.

RD20 participates in long-lasting stomatal control and in drought tolerance

It is well established that ABA promotes water deficit tolerance in plants through stomatal regulation (Schroeder et al. 2001, Finkelstein and Rock 2002). In this work, we report that *RD20* is up-regulated by dehydration in an ABA-dependent manner; furthermore, the analysis of *pRD20::GUS* reporter transgenic lines revealed that *RD20* gene expression occurs in guard cells, suggesting that RD20 may be involved in the regulation of plant water status in response to drought. Thus, transpirational water losses of *rd20*, ORK5 and the WT were determined at the whole-plant level in two conditions (**Fig. 5**). In the well-watered condition, soil relative water content (RWC) was 35%, whereas in water deficit condition, RWC was 20%. As expected, transpiration rates were significantly reduced in plants submitted to soil water deficit and, more interestingly, *rd20* plants were inclined to lose more water than WT and ORK5 plants, notably in water deficit conditions (**Fig. 5A**). Automated daily pictures of each plant were taken throughout the duration of the transpiration experiment to calculate the leaf expansion rate (ER). ER was significantly reduced by water deficit in all genotypes (**Fig. 5B**). However, it was systematically lower in the *rd20* mutant and significantly higher in the complemented ORK5 line under water deficit compared with KO plants (**Fig. 5B**). Non-destructive estimation of transpiration and ERs allowed the calculation of water use efficiency (WUE), expressed as rosette area increment per unit soil water used, for the different genotypes (**Fig. 5C**). WUE significantly increased under water deficit compared with well-watered conditions for all genotypes. Additionally, upon water deficit, combining slightly higher transpiration and more severely reduced growth in *rd20* mutant compared with WT plants led to a significantly lower WUE in *rd20* (**Fig. 5C**). This difference in WUE is not due to stomatal cell density which does not differ significantly among genotypes (**Supplementary Fig. S2**). Differences in WUE between genotypes were not accompanied by any contrast in the final size of the aerial part of the plants. Total leaf number, rosette fresh weight and specific rosette area at bolting were reduced by water deficit to a similar extent for all genotypes (**Supplementary Fig. S2**). Finally, to evaluate the allocation to below-ground parts, the root–shoot ratio was calculated. This ratio was significantly increased in response to water deficit in a similar way for all genotypes (**Fig. 5D**).

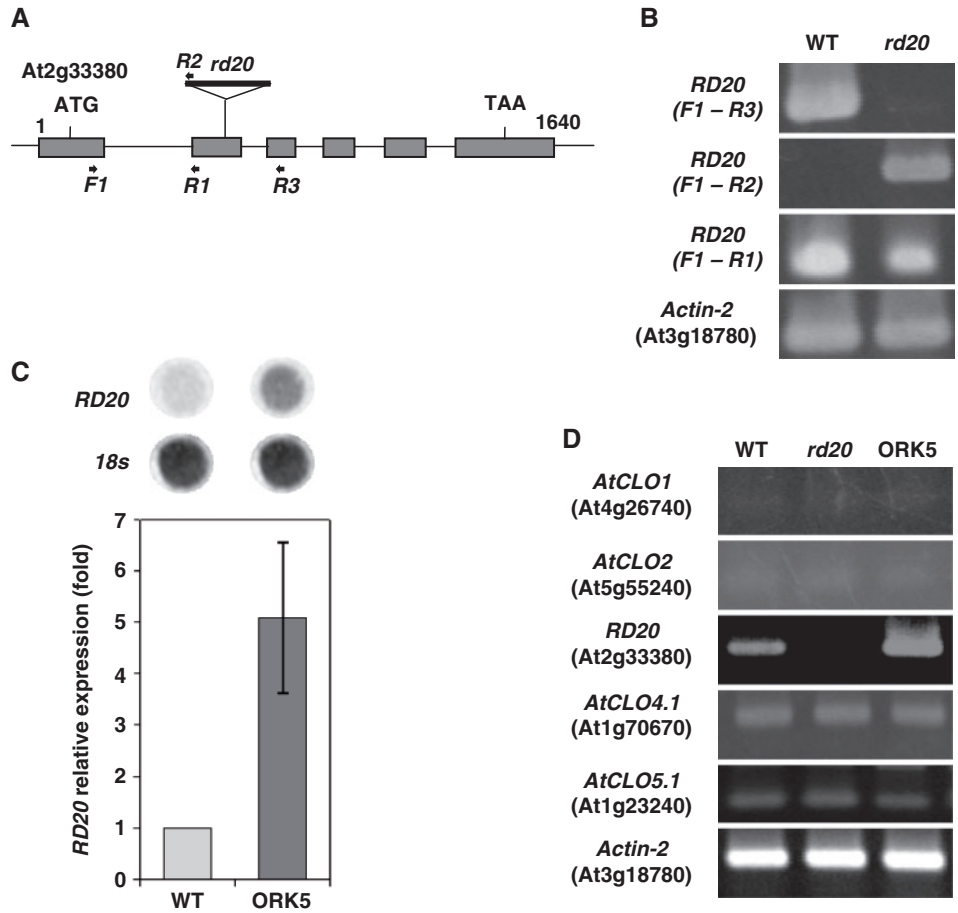

Fig. 4 (A and B) Molecular characterization of the *rd20* T-DNA insertional mutant. (A) Scheme of the *rd20* T-DNA insertional mutant. The intron–exon organization of the Arabidopsis *RD20* gene is depicted by lines and boxes, respectively. The position of the T-DNA insertion is indicated by a thick black line (not drawn to scale). The positions of the primers used for PCR and RT–PCR amplifications are indicated by arrows. (B) Expression levels of *RD20* mRNA in the WT and the *rd20* mutant as determined by RT–PCR. Total RNA was extracted from 4-week-old plants left without irrigation for 7 d and analyzed by RT–PCR using specific primers. *Actin-2* (At3g18780) served as a control for RNA integrity, and as a semi-quantitative standard. (C) *RD20* gene expression in the complemented *rd20* KO mutant line ORK5. Dot-blot results are shown in the upper panel and quantification analyses in the lower panel. The error bar represents the SD. (D) *AtCLO1-5* gene expression profile. Total RNA from 4-week-old leaves was extracted from WT, *rd20* and ORK5 transgenic lines grown in well-watered conditions. RNAs were analyzed by semi-quantitative RT–PCR using gene-specific primers corresponding to *AtCLO1*, *2*, *3*(*RD20*), *4.1* and *5.1* genes. *Actin-2* (At3g18780) served as a control for RNA integrity, and as a semi-quantitative standard

Considering that RD20 expression occurs essentially in aerial tissues, in stomatal guard cells and in response to ABA, the weak increase in transpiration of *rd20* mutant plants questions the role of RD20 in the regulation of stomatal movements. Because transpiration causes leaf cooling, measurement of leaf temperature using infrared thermal imaging gives an estimation of leaf transpiration (Merlot et al. 2002). Using infrared thermography, we showed that *rd20* plants display a low but significant decrease in leaf temperature compared with WT and ORK5 plants (**Supplementary Fig. S3**). As a control, the OPEN STOMATA2 mutant was used to calibrate the experiment (Merlot et al. 2007) and, although differences between *rd20*, WT and ORK5 are weak compared with *ost2*, they are significant enough to support the hypothesis that RD20 contributes to the regulation of stomatal movements. To explore the role of RD20 in the control of stomatal movement further, a detailed analysis of stomatal aperture was performed on WT, *rd20* and ORK5 plants (**Fig. 6**). Light-induced stomatal opening was investigated, and indicated that *rd20* mutant plants exhibited a significant increase in stomatal aperture as compared with WT and ORK5 plants. ORK5 displayed a WT response to light-induced stomatal opening. ABA-mediated inhibition of stomatal opening was also evaluated on epidermal peels incubated in the presence or absence of 10 μM ABA. The results showed that *rd20* stomata were less sensitive than those of the WT and that ORK5 plants exhibited an enhanced response to ABA-mediated inhibition of stomatal opening (**Fig. 6B**). These results prompted us to study the effect of fusicoccin, a fungal toxin inducing stomatal opening (Gomarsca et al. 1993), to determine precisely the action of RD20 in relation to

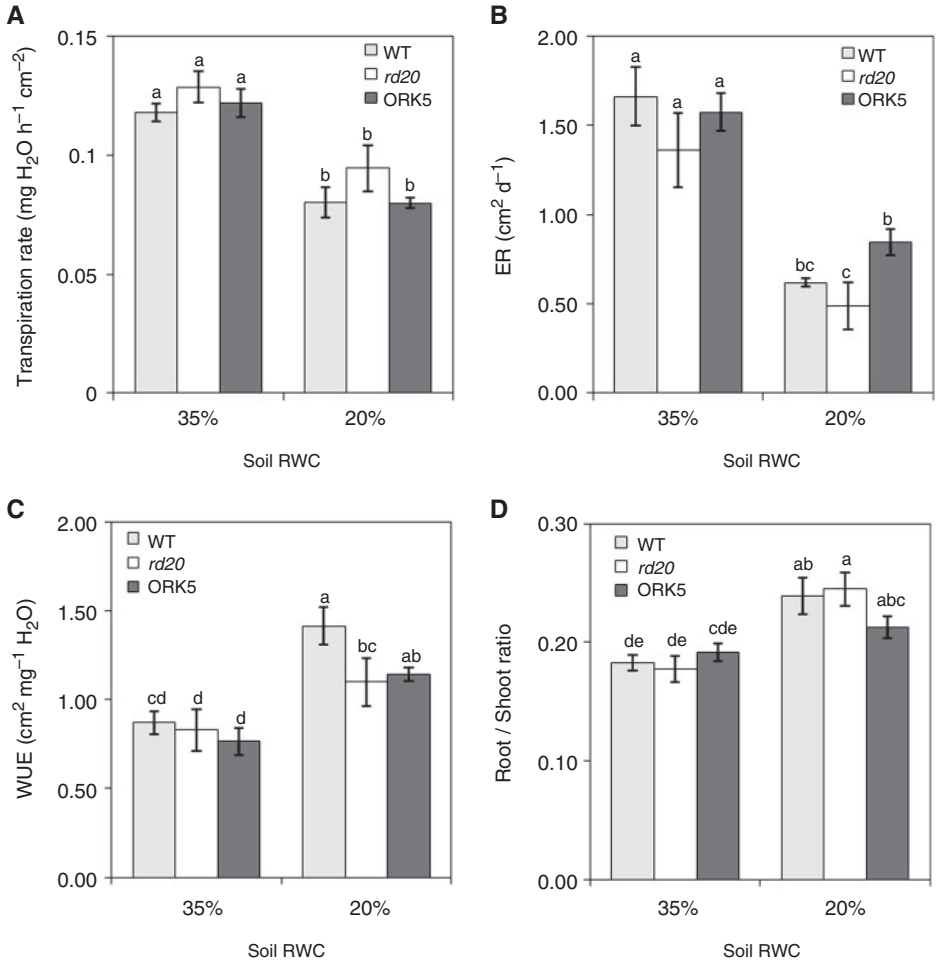

Fig. 5 Effect of the soil relative water content (RWC) on whole plant transpiration dynamics, expansion rate (ER), water use efficiency (WUE) and root–shoot ratio (A–D) of WT, *rd20* and ORK5 transgenic plants. The data are the mean of two independent experiments (±SEM). Bars labeled with different letters (a–e) indicate statistically significant differences between genotypes ($P < 0.05$) using the unplanned Kruskal–Wallis multiple comparisons test.

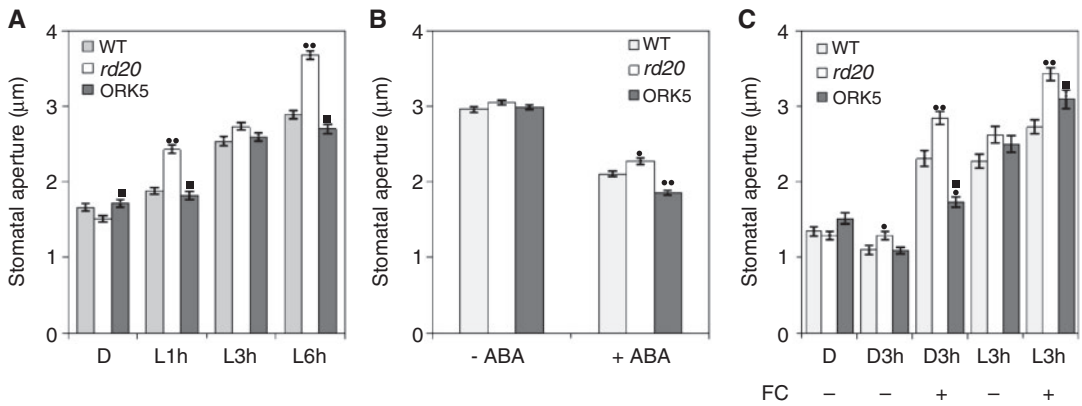

Fig. 6 Regulation of stomatal aperture by light, ABA and fusicoccin (FC). (A) Stomatal opening kinetics in response to light. Epidermal strips were incubated for 30 min in the dark to promote maximal stomatal closure (D) and were subsequently exposed to light for the indicated time. (B) Inhibition of light-induced stomatal opening by 10 µM ABA. Measurements were performed after 3 h of light exposure. (C) Induction of stomatal opening by 5 µM FC. Stomatal apertures are measured after 30 min of incubation in the dark without FC (D) or after 3 h of incubation in the dark (D3h) or in the light (L3h) in the absence or presence of 5 µM FC. Data presented are the mean of three independent experiments (±SEM) of at least 360 stomata. Single and double filled circles indicate significant differences from the WT ($P < 0.01$ and $P < 0.0001$, respectively); a filled square indicates significant differences between *rd20* KO plants and ORK5 plants ($P < 0.01$).

the plasma membrane H^+-ATPase. The *rd20* KO plants exhibited hypersensitive fusicoccin-induced stomatal opening in the dark as well as in the light as compared with WT and ORK5 plants (**Fig. 6C**). ORK5 plants were less sensitive than WT plants to fusicoccin-induced stomatal opening in the dark but exhibited a WT response in the light condition. Altogether, these data support that RD20 is involved in a long time scale regulation of plant water status, and suggest that RD20 may act downstream of the plasma membrane H^+-ATPase. These differences in stomatal aperture regulation could explain differences in transpiration, ERs and WUE.

Finally, we evaluated the behavior of WT, *rd20* and ORK5 mutant plants in response to drought. Compared with previous work using the PHENOPSIS automaton where stable soil water content was imposed, drought tolerance assays were performed on 4-week-old plants previously irrigated with water every 3 d before a complete arrest of irrigation. Plants were observed daily and, after 6 d, mutant plants exhibited more pronounced wilting symptoms than the WT (**Fig. 7**). After a 10 d water stress period, re-watering the pots led to a better survival of WT compared with the *rd20* mutant plants. Concerning the behavior of the overexpressing complemented ORK5 line, the wilting symptoms were similar to those of the WT (data not illustrated). Because differences were only observed for KO plants, we evaluated in parallel the impact of the overexpression of *RD20* in another Arabidopsis accession (Col-8) using all the tests described in this work. No significant differences were observed between WT and overexpressing Col-8 lines (not shown), indicating that overexpression of *RD20* is not sufficient to improve drought tolerance significantly. Several works reported that *RD20* is also highly induced by NaCl treatment (Takahashi et al. 2000, Kreps et al. 2002, Kant et al. 2008), and this raises the question of the role of RD20 in salt stress responses. Thus we investigated the behavior of *rd20* and WT plants in response to 150 mM NaCl treatment (**Supplementary Fig. S4**). After 3 weeks, the number of senescent leaves was significantly higher in *rd20* KO plants compared with WT plants, indicating that *rd20* KO plants are also more sensitive to salt stress than the WT. This result indicates that *RD20* participates in water deficit as well as in salt stress responses.

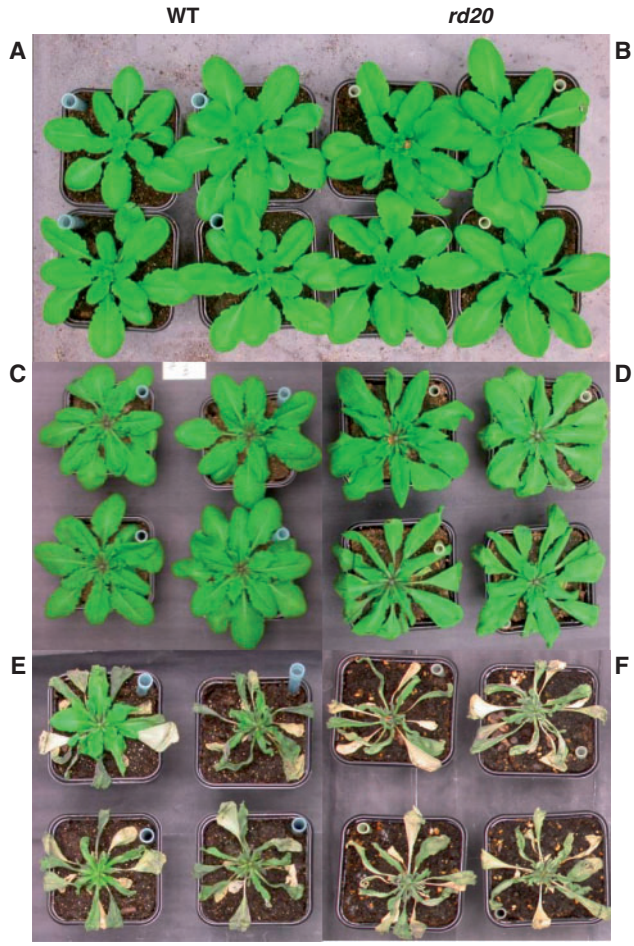

Fig. 7 *RD20* mutation impairs drought responses. Analysis of drought effects on WT (A, C, E) and *rd20* mutant (B, D, F) adult Arabidopsis plants. (A and B) Four-week-old plant before stopping irrigation; (C and D), plants 10 d after stopping irrigation; (E and F), photographs of plants 10 d after re-watering the pots.

Discussion

RD20, an OB-associated protein, is the only caleosin induced by abiotic stresses

The aim of this work was to evaluate the role of RD20, a stress-induced caleosin from Arabidopsis. For this purpose, we first analyzed the subcellular localization of RD20 using transient expression of a RD20–GFP–GUS fusion protein in onion epidermal cells and showed that RD20, like AtCLO1 and AtCLO2, is an OB-associated protein. However, at the gene expression level, RD20's profile is quite different from that of other caleosins. RD20 is expressed in particular tissues or organs during plant development and is induced in a rapid and a transient manner by dehydration and ABA, suggesting that RD20 is part of an abiotic stress-related signaling pathway. A search for *cis*-acting elements related to ABA and drought responses was performed in the *RD20* promoter region as well as in other caleosin sequences using the Arabidopsis Gene Regulatory Information Server (http://arabidopsis.med.ohio-state.edu/). The results indicated that the ABRE (ABA-responsive element), ABRE-like and DRE (dehydration-responsive element) *cis*-elements are over-represented in the *RD20* promoter sequence compared with the other Arabidopsis caleosin genes (**Supplementary Table S2**). This analysis also points out that the *RD20* promoter region exhibits a significant enrichment in AtMYC2-binding sites, while none is observed in the other caleosin gene promoter sequences. Interestingly, AtMYC2 acts as a positive regulator of ABA signaling under drought stress (Abe et al. 2003). Concerning the regulation of *RD20* gene expression during development, it can be correlated to the *RD20* induction by ABA. For instance, the presence of ABRE/CBF2-binding sites that are associated with leaf senescence and

ABA responses (Sharabi Swager et al. 2010) could explain the expression pattern of RD20 in mature flowers. Otherwise, because ABA is a known regulator of seed maturation (Finkelstein and Rock 2002), it is also reasonable to visualize GUS activity in young siliques. In response to wounding, we showed that *RD20* gene expression increases rapidly but it is limited to the wounding sites (**Supplementary Fig. S1**). Knowing that wounding provokes desiccation of wounded tissues and that ABA is necessary to produce a full wounding response (Hillwig et al. 2008), we propose that *RD20* gene induction at wounding sites results from ABA-dependent processes. Finally, although *RD20* gene expression is up-regulated in response to salt stress (Takahashi et al. 2000) and in transgenic plants overexpressing a constitutive active form of the salt stress-responsive transcription factor AtbZIP17 (Liu et al. 2008), no AtbZIP17-binding element was found in the *RD20* promoter sequence. Collectively, this indicates that *RD20* is an ABA- and drought stress-associated caleosin and this is supported by the presence of ABA- and abiotic stress-responsive *cis*-acting elements in its promoter region.

Microarray data represent a mine of information on gene regulation and can be used to identify co-regulated gene networks (Manfield et al. 2006). Such analyses performed with Arabidopsis caleosins revealed that RD20 is poorly co-regulated with AtCLO1 and AtCLO2, suggesting that it probably plays different biological roles (**Supplementary Fig. S5**). This analysis also points out that AtCLO1 and AtCLO2 display a strong co-regulation. Hanano et al. (2006) demonstrated that AtCLO1 and AtCLO2 possess a peroxygenase activity. Even though these two proteins share a similar expression profile and common enzymatic activity, their biological functions are not fully redundant because a single mutation in *AtCLO1* leads to a growth defect compared with WT plants at the onset of germination (Poxleitner et al. 2006). These data strongly suggest that although several caleosins are present in Arabidopsis, each may fulfill specific functions at the spatial and temporal level during plant development and/or in response to environmental stresses. Peroxygenase activity of AtCLO1 and AtCLO2 requires the presence of calcium and two conserved histidines. Sequence alignment of RD20 with AtCLO1 and AtCLO2 reveals that these two histidines are present in the RD20 sequence, and previous work by Takahashi et al. (2000) showed that RD20 is able to bind calcium. Overall, these data and the OB localization of RD20 support a putative peroxygenase activity for RD20 and suggest a role in lipid modification and/or degradation as proposed for AtCLO1 and AtCLO2 (Poxleitner et al. 2006). Involvement of maize peroxygenase activity in cuticle and wax synthesis has been proposed by Lequeu et al. (2003). The synthesis of cuticle and cuticular waxes is enhanced by water deficit conditions and ABA, and they are proposed to prevent water losses (Kosma et al. 2009). Moreover, increasing evidence indicates that lipids can act as mediators in many physiological processes such as growth, differentiation, and biotic and abiotic stress responses (Wang 2004). For instance, drought is able to trigger phosphatidic acid production that mimics ABA action (Testerink and Munnik 2005). Interestingly, Coca and San Segundo (2010) report that CPK1, a calcium-dependent protein kinase associated with OBs, mediates pathogen resistance in Arabidopsis. This work clearly shows that OBs that are found in most plant cells cannot be considered only as storage lipid organelles present in seeds. Our knowledge is still scarce on the role of lipid bodies, but this work paves the way for a better understanding of the function of this organelle and of the associated proteins in plant stress responses. Collectively, considering that RD20 acts as a putative OB-associated peroxygenase, it might contribute to lipid signaling/modifications in plant stress responses.

Mutation in RD20 alters stomatal aperture and drought tolerance

To understand the role of RD20, a loss-of-function strategy was developed using KO and complemented *RD20*-overexpressing transgenic lines. We showed that *RD20* gene expression is strongly induced by ABA and occurred in guard cells, as reported by the transcriptome analysis of guard cells and mesophyll cells (Leonhardt et al. 2004). Thus, we evaluated the contribution of RD20 to the regulation of plant water status in drought conditions and showed that transpiration rates decreased in all genotypes. As noticed before, water losses were slightly greater in *rd20* plants and the ER and WUE were lower in the *rd20* mutant compared with the WT under water deficit. To our knowledge, only two genes (*ERECTA* and *GPA1*) have been identified as regulators of WUE in Arabidopsis (Masle et al. 2005, Nilson and Assmann 2010). However, multiple WUE-associated loci have been identified, indicating that WUE is controlled by a complex genetic network (Juenger et al. 2005). Differences in transpiration rate and WUE in *rd20* KO plants prompted us to compare the stomatal regulation in WT, *rd20* KO and ORK5 plants. Unlike OST2 (Merlot et al. 2007), RD20 cannot be considered as a major actor in stomatal regulation. However, using leaf temperature imaging and measurements of stomatal aperture on epidermal strips, we showed that RD20 contributes to stomatal regulation. Both methods indicated that *rd20* KO plants display an enhanced stomatal aperture and transpiration compared with the WT and ORK5. These results are in agreement with data presented in **Fig. 7** showing that mutation in *RD20* finally impacts drought tolerance as compared with WT plants. It is clearly established that stomatal opening results from the uptake of solutes and cations into the cytosol and this uptake is mediated by H^+-ATPase-dependent hyperpolarization of the plasma membrane (Kwak et al. 2008). Activation of the plasma membrane H^+-ATPase by fusicoccin allowed us to determine that RD20 acts downstream of the plasma membrane H^+-ATPase. The results indicated that loss of RD20 is not compensated by other caleosins, as was suggested by the gene expression patterns of caleosins. However, we also showed that overexpression of *RD20* is not sufficient to enhanced tolerance to drought, supporting that even if RD20 participates in drought tolerance, it cannot be considered as a limiting component

and that other elements are required to enhance tolerance to water deficit. We also showed that the role of RD20 is not limited to drought tolerance. RD20 plays a positive role in salt stress response and, knowing that the *RD20* gene is induced by various abiotic stresses such as drought, salt stress, cold and wounding (Kant et al. 2008), we can hypothesize that RD20 acts in a stress signaling hub that sets up multiple abiotic responses.

In the present study, we combined whole plant physiology and molecular/genetic approaches to show that RD20, an ABA-responsive gene, participates in drought tolerance mechanisms through the regulation of stomatal aperture, plant growth and WUE. Finally, like ERECTA, GPA1 and a WUE quantitative trait locus identified by Juenger et al. (2005), *RD20* is located at the bottom of chromosome 2, a region that appears to be important in the regulation of plant transpiration efficiency in Arabidopsis.

Materials and Methods

Plant material, growth conditions and stimulus treatments

Seeds from *Arabidopsis thaliana* ecotype Wassilewskija (Ws-4) and mutant lines which were ABA deficient [*aba1-5* (Col)] and ABA insensitive [*abi1-1* (Ler)] were purchased from the Nottingham Arabidopsis Stock Centre. A T-DNA insertional mutant line impaired in *RD20* (At2g33380) [*rd20* (Ws-4)] was obtained from INRA Versailles. To avoid variations in seed quality, all the seeds were harvested from plants cultivated in identical conditions over the same time period. Growth experiments were performed in the PHENOPSIS automaton to impose stable and reproducible soil water content treatments in the same controlled micrometeorological conditions (Granier et al. 2006). Two soil water contents were imposed (0.35 or 0.2 g H_2O g^{-1} dry soil), corresponding to optimal plant growth and continuous moderate water deficit conditions, respectively (Aguirrezabal et al. 2006). Seeds were sown in pots (200 ml) filled with a mixture (1:1, v/v) of a loamy soil and organic compost. Soil water content was determined at sowing to estimate the initial amount of dry soil and water in each pot. This allowed the soil water content of each pot to be maintained at precisely defined levels using a modified one-tenth strength Hoagland solution to compensate for daily water losses (Tisné et al. 2008). Water deficit treatments started when leaf 2 had appeared. Plants were used for measurement of morphological traits, growth and transpiration, and to determine WUE. Drought assays were performed with 4-week-old plants grown in soil in the growth chamber. Plants were irrigated with water every 3 d and watering was withheld for 10 d before re-watering the pots for plant survival analysis. To minimize experimental variations, the WT and mutants were randomly placed on the same tray. The experiment was repeated three times and results from one representative experiment are shown.

Subcellular localization of a *Promoter 35S::RD20$_{cDNA}$-GFP-GUS* fusion

A *P35S::RD20$_{cDNA}$_GFP_uidA* was obtained as previously described (Perruc et al. 2004) using a full-length RD20 cDNA clone (RAFL06-69-K02, AY063964) purchased from Riken and the *pRJG23* vector (Grebenok et al. 1997). A *P35S::GFP_uidA* construct was obtained and used as a cytoplasmic control (Perruc et al. 2004). Both constructs were introduced into onion epidermal cells with a helium biolistic particle delivery system (Bio-Rad), and expression of the fusion constructs was observed after 24 h by fluorescence microscopy using an SP2 confocal laser scanning system. The 488 nm line of the argon laser was used for excitation, and images were obtained in the range 500–530 nm corresponding to the GFP emission range. *P35s::RD20$_{cDNA}$_GFP_uidA*-transformed onion epidermal cells were stained with the neutral lipid dye Nile red for OB visualization (Greenspan et al. 1985). Z-scan series within the thickness of the samples were acquired to determine if the emitted fluorescence was restricted or not in a given cell compartment.

Generation and analysis of *RD20 promoter-GUS* expression transgenic lines

To generate the *RD20 promoter::uidA* construct (*pRD20::GUS*), a 1.5 kb *RD20* promoter sequence was PCR amplified from the F4P9 bacterial artificial chromosome (BAC; ABRC) using the *Gat_ProRD20_F* and *Gat_ProRD20_R* primers (**Supplementary Table S1**). PCR products were further amplified and cloned into the *pDONR207* vector (Invitrogen) before a further recombination into the destination vector *pMDC162* according to Gateway® technology. We also designed a construct made of the 1.5 kb *RD20 promoter*, the entire *RD20* coding region including introns and the GUS reporter coding sequence (*pRD20::RD20$_{gDNA}$_GUS*). The sequence was amplified from the F4P9 BAC clone using the *Gat_ProRD20_F* and *Gat_ProRD20g_GUS* primers (**Supplementary Table S1**) and used to create the expression construct in the *pMDC164* vector (Curtis and Grossniklauss 2003). The constructs were introduced into *Agrobacterium tumefaciens* C58 before transformation of Arabidopsis WT [Col-8] plants by floral dipping (Clough and Bent 1998). For GUS staining, various tissues from T_3 transgenic reporter lines were treated as reported by Magnan et al. (2008).

Gene expression analysis

Real-time RT–PCR analyses of *RD20* and *RAB18* gene expression were performed as described by Magnan et al. (2008). Total RNA were prepared using the Nucleospin RNA kit (Macherey-Nagel) from the WT, the ABA-deficient mutant *aba1-5* and the ABA-insensitive mutant *abi1-1* subjected to dehydration or to 100 µM ABA. A 1 µg aliquot of RNA was subjected to reverse transcription using Superscript II (Invitrogen). Quantitative PCR was run on a Roche Lightcycler system according to the manufacturer's recommendations. The suitability of the primer sets and the specificity and identity of the RT–PCR products were monitored by melting curve analysis of the PCR products.

Transcript levels of *β-tubulin* and an external mRNA, *desmin*, were used for standardization. Two biological and three technical replicas were performed. The PCR primer sets used are listed in **Supplementary Table S1**. Gene expression of *RD20*, *AtCLO1* (At4g26740), *AtCLO2* (At5g55240), *AtCLO4.1* (At1g70670) and *AtCLO5.1* (At1g23240) was also determined by semi-quantitative RT–PCR using specific primers (**Supplementary Table S1**). The expression level of *Actin-2* (At3g18780) served as a quantifying control.

Molecular characterization of the *rd20* mutant and complemented lines

PCR assays were performed on genomic DNA from the WT and the *rd20* mutant to evaluate the allelic state of T-DNA in the *RD20* gene (**Fig. 4**). Detection of *RD20* transcripts was performed by RT–PCR on total RNA. A 1 µg aliquot of RNA was subjected to reverse transcription using Superscript II (Invitrogen) and PCR amplifications were performed using two sets of *RD20*-specific primers *F1-F2* and *F1-R3* (**Supplementary Table S1**), allowing the detection of full-length or truncated RD20 transcripts. The expression level of *Actin-2* (At3g18780) served as a quantifying control. After 40 PCR cycles, amplified products were resolved by gel electrophoresis. To generate complemented KO *rd20* plants, the *P35S::RD20*$_{cDNA}$ construct was obtained from the full-length *RD20* cDNA clone. PCR amplifications with the *35S_GST_RD20B1* and *35S_GST_RD20B2* primers (**Supplementary Table S1**) were performed and PCR products were used to create the expression cassette in the *pMDC32* vector and introduced into Arabidopsis *rd20* KO plants. Quantification of the *RD20* level in these plants was performed by dot-blot using 5 or 1 µg of RNA hybridized with ^{32}P-labeled cDNA probes prepared from *RD20* cDNA or 18S rRNA as a loading control. Hybridization signals were quantified using a PhosphorImager.

Transpiration rate, absolute growth rate and water use efficiency

Using the PHENOPSIS phenotyping platform, at least six plants per genotype were followed to determine transpirational water loss in optimal and water deficit conditions (0.35 and 0.20 g H_2O g^{-1} dry soil, respectively). Plant water loss was monitored by successive weighing of the pots every 2–4 h over 3–4 days and nights when plants had reached the bolting stage (stage 5.10 of Boyes et al. 2001). Soil evaporation was prevented by sealing the pot surface below the rosettes with four layers of plastic film. The whole plant transpiration rate (mg h^{-1}) was estimated as the slope of the linear relationship between weight and time during the whole time period of measurement. Projected rosette area (cm^2) was determined daily by vertical photographs. Plants were then harvested and total rosette fresh weight and total (dissected) leaf area of the rosette (cm^2) were measured. Transpirational water loss was then expressed per rosette area (mg H_2O h^{-1} cm^{-2}). WUE (cm^2 mg^{-1} H_2O) was estimated non-destructively as the rate of rosette area expansion (ER, cm^2 d^{-1}) per unit loss of water during the experiment.

Stomatal aperture measurement

Leaves from well-watered 3- to 4-week-old plants were harvested in darkness at the end of the night period. Stomatal aperture measurements were performed on epidermal strips, incubated in 30 mM KCl, 10 mM MES-KOH, pH 6.5, at 22°C, and exposed to light (300 µmol m^{-2} s^{-1}). Stomatal apertures were measured using a Nikon Optiphot-2 microscope (http://www.nikon.com/) fitted with a digital camera and a TG 1017 digitizing table (Houston Instruments; http://www.tms-plotters.com) linked to a personal computer. To study ABA-induced inhibition of stomatal opening, epidermal strips were incubated for 3 h in the light in the presence or absence of 10 µM ABA. The induction of stomatal opening was also performed in the presence of fusicoccin, a fungal toxin known to activate the plasma membrane H^+-ATPase promoting stomatal opening (Gomorasca et al. 1993). Epidermal strips were incubated for 3 h either in the dark or in the light in the absence or presence of 5 µM fusicoccin prior to stomatal aperture measurement. For each treatment, at least 60 stomatal apertures were measured in <5 min. Data presented are the mean of at least three independent experiments.

Statistical analyses

All statistical analyses were performed using the non-parametric procedure of Kruskal–Wallis for multiple comparisons. All statistical analyses were performed using R (http://www.R-project.org).

Supplementary data

Supplementary data are available at PCP online.

Funding

This work was supported by the University Paul Sabatier (Toulouse III); the Centre National de la Recherche Scientifique (CNRS); Institut National de la Recherche Agronomique (INRA); Commissariat à l'Energie Atomique (CEA); Agence Nationale de la Recherche (ANR) [grant No. ANR-06-BLAN-0122]; the French Ministry of National Education and Research [to Y.A.].

Acknowledgments

We thank the technical services for plant material and technical assistance, M. Charpenteau, C. Lachaud, E. Kerdaffrec and A. Jauneau for their contribution to this work, the Riken Bioresource Center, the Arabidopsis Biological Resource Center for providing cDNA and genomic Arabidopsis clones, the Nottingham Arabidopsis Stock Center, and INRA for Arabidopsis mutant lines.

References

Abe, H., Urao, T., Ito, T., Seki, M., Shinozaki, K. and Yamaguchi-Shinozaki, K. (2003) Arabidopsis AtMYC2 (bHLH) and AtMYB2 (MYB) function as transcriptional activators in abscisic acid signaling. *Plant Cell* 15: 63–78.

Abell, B.M., Holbrook, L.A., Abenes, M., Murphy, D.J., Hills, M.J. and Moloney, M.M. (1997) Role of the proline knot motif in oleosin endoplasmic reticulum topology and oil body targeting. *Plant Cell* 9: 1481–1493.

Aguirrezabal, L., Bouchier-Combaud, S., Radziejwoski, A., Dauzat, M., Cookson, S.J. and Granier, C. (2006) Plasticity to soil water deficit in *Arabidopsis thaliana*: dissection of leaf development into underlying growth dynamic and cellular variables reveals invisible phenotypes. *Plant Cell Environ.* 29: 2216–2227.

Alexandre, C., Möller-Steinbach, Y., Schönrock, N., Gruissem, W. and Hennig, L. (2009) Arabidopsis MSI1 is required for negative regulation of the response to drought stress. *Mol. Plant* 2: 675–687.

Bartels, D. and Sunkar, R. (2005) Drought and salt tolerance in plants. *Crit. Rev. Plant Sci.* 24: 23–58.

Boyes, D.C., Zayed, A.M., Ascenzi, R., McCaskill, A.J., Hoffman, N.E., Davis, K.R., et al. (2001) Growth stage-based phenotypic analysis of Arabidospis: a model for high throughput functional genomics in plants. *Plant Cell* 13: 1499–1510.

Bray, E.A. (2004) Genes commonly regulated by water-deficit stress in *Arabidopsis thaliana*. *J. Exp. Bot.* 55: 2231–2341.

Chen, J.C.F. and Tzen, J.T.C. (2001) An in vitro system to examine the effective phospholipids and structural domain for protein targeting to seed oil bodies. *Plant Cell Physiol.* 42: 1245–1252.

Clough, S.J. and Bent, A.F. (1998) Floral dip: a simplified method for *Agrobacterium*-mediated transformation of *Arabidopsis thaliana*. *Plant J.* 16: 735–743.

Coca, M. and San Segundo, B. (2010) AtCPK1 calcium-dependent protein kinase mediates pathogen resistance in Arabidopsis. *Plant J.* 63: 526–540.

Curtis, M.D. and Grossniklaus, U. (2003) A gateway cloning vector set for high-throughput functional analysis of genes in planta. *Plant Physiol.* 133: 462–469.

Finkelstein, R.R. and Rock, C.D. (2002) Abscisic acid biosynthesis and response. *In* The Arabidopsis Book. Edited by Sommerville, C.R. and Meyerowitz, E.M. pp. 1–48. American Society of Plant Biologists, Rockville, MD.

Frandsen, G., Müller-Uri, F., Nielsen, M., Mundy, J. and Skriver, K. (1996) Novel plant Ca^{2+} binding protein expressed in response to abscisic acid and osmotic stress. *J. Biol. Chem.* 271: 343–348.

Gomarasca, S., Vannini, C., Venegoni, A., Talarico, A., Marrè, M.T. and Soave, C. (1993) A mutant of *Arabidopsis thaliana* with reduced response to fusicoccin. *Plant Physiol.* 103: 165–170.

Granier, C., Aguirrezabal, L., Chenu, K., Cookson, S.J., Dauzat, M., Hamard, P., et al. (2006) PHENOPSIS, an automated platform for reproducible phenotyping of plant responses to soil water deficit in *Arabidopsis thaliana* permitted the identification of an accession with low sensitivity to soil water deficit. *New Phytol.* 169: 623–635.

Grebenok, R.J., Pierson, E., Lambert, G.M., Gong, F.-C., Afonso, C.L., Haldeman-Cahill, R., et al. (1997) Green-fluorescent protein fusions for efficient characterization of nuclear targeting. *Plant J.* 11: 573–586.

Greenspan, P., Mayer, E.P. and Fowler, S.D. (1985) Nile Red: a selective fluorescent stain for intracellular lipid droplets. *J. Cell Biol.* 100: 965–973.

Hanano, A., Burcklen, M., Flenet, M., Ivancich, A., Louwagie, M., Garin, J., et al. (2006) Plant seed peroxygenase is an original heme-oxygenase with an EF-hand calcium binding motif. *J. Biol. Chem.* 281: 33140–33151.

Hillwig, M.S., Lebrasseur N.D., Green, P.J. and Macintosh, G.C. (2008) Impact of transcriptional, ABA-dependent, and ABA-independent pathways on wounding regulation of RNS1 expression. *Mol. Genet. Genomics* 280: 249–261.

Hruz, T., Laule, O., Szabo, G., Wessendorp, F., Bleuler, S., Oertle, L., et al. (2008) Genevestigator V3: a reference expression database for the meta-analysis of transcriptomes. *Adv. Bioinformatics* 2008: 420747.

Juenger, T.E., McKay, J.K., Hausmann, N., Tjes, J.J.B., Sen, S., Stowe, K.A., et al. (2005) Identification and characterization of QTL underlying whole-plant physiology in *Arabidopsis thaliana*: $\delta^{13}C$, stomatal conductance and transpiration efficiency. *Plant Cell Environ.* 28: 697–708.

Kant, P., Gordon, M., Kant, S., Zolla, G., Daydov, O., Heimer, Y.M., et al. (2008) Functional-genomics-based identification of genes that regulate Arabidopsis responses to multiple abiotic stresses. *Plant Cell Environ.* 31: 697–714.

Kosma, D.K., Bourdenx, B., Bernard, A., Parsons, E.P., Lü, S., Joubès, J., et al. (2009) The impact of water deficit on leaf cuticle lipids of Arabidopsis. *Plant Physiol.* 151: 1918–1929.

Kreps, J.A., Wu, Y., Chang, H.-S., Zhu, T., Wang, X. and Harper, J.F. (2002) Transcriptome changes for Arabidopsis in response to salt, osmotic and cold stress. *Plant Physiol.* 130: 2129–2141.

Kwak, J.M., Mäser, P. and Schroeder, J.I. (2008) The clickable guard cell, version II: integrative model of guard cell transduction mechanisms and pathways. *In* The Arabidopsis Book. doi: 10.1199/tab.0114

Lang, V. and Palva, E.T. (1992) The expression of a *rab*-related gene, *rab18*, is induced by abscisic acid during the cold acclimation process of *Arabidopsis thaliana* (L.) Heynh. *Plant Mol. Biol.* 20: 951–962.

Leonhardt, N., Kwak, J.M., Robert, N., Waner, D., Leonhardt, G. and Schroeder, J.I. (2004) Microarray expression analyses of Arabidopsis guard cells and isolation of a recessive abscisic acid hypersensitive protein phosphatase 2C mutant. *Plant Cell* 16: 596–615.

Lequeu, J., Fauconnier, M., Chammai, A., Bronner, R. and Blée, E. (2003) Formation of plant cuticle: evidence for the occurrence of the peroxygenase pathway. *Plant J.* 36: 155–184.

Liu, J.X., Srivastava, R. and Howell, S.H. (2008) Stress-induced expression of an activated form of AtbZIP17 provides protection from salt stress in Arabidopsis. *Plant Cell Environ.* 31: 1735–1743.

Magnan, F., Ranty, B., Charpenteau, M., Sotta, B., Galaud, J.P. and Aldon, D. (2008) Mutations in *AtCML9*, a calmodulin-like protein from *Arabidopsis thaliana*, alter plant responses to abiotic stress and abscisic acid. *Plant J.* 56: 575–589.

Manfield, I.W., Jen, C.-H., Pinney, J.W., Michalopoulos, I., Bradford, J.R., Gilmartin, P.M., et al. (2006) Arabidopsis co-expression tool (ACT): web-server tools for microarray-based gene expression analysis. *Nucleic Acids Res.* 34: W504–W509.

Masle, J., Gilmore, S.R. and Farquhar, G.D. (2005) The ERECTA gene regulates plant transpiration efficiency in Arabidopsis. *Nature* 436: 866–870.

Merlot, S., Leonhardt, N., Fenzi, F., Valon, C., Costa, M., Piette, L., et al. (2007) Constitutive activation of a plasma membrane H(+)-ATPase prevents abscisic acid-mediated stomatal closure. *EMBO J.* 26: 3216–3226.

Merlot, S., Mustilli, A.-C., Genty, B., North, H., Lefebvre, V., Sotta, B., et al. (2002) Use of infrared thermal imaging to isolate Arabidopsis mutants defective in stomatal regulation. *Plant J.* 30: 601–609.

Murphy, D.J., Hernandez-Pizon, I. and Patel, K. (2001) Role of lipid-bodies and lipid-body proteins in seeds and other tissues. *J. Plant Physiol.* 158: 471–478.

Naested, H., Frandsen, G.I., Jauh, G.-Y., Hernandez-Pinzon, I., Nielsen, H.B. and Murphy, D.J. (2000) Caleosins: Ca^{2+} binding proteins associated with lipid bodies. *Plant Mol. Biol.* 44: 436–476.

Nilson, S.E. and Assmann, S.M. (2010) The α-subunit of the Arabidopsis heterotrimeric G protein, GPA1, is a regulator of transpiration efficiency. *Plant Physiol.* 152: 2067–2077.

Oono, Y., Seki, M., Nanjo, T., Narusaka, M., Fujita, M., Satoh, R., et al. (2003) Monitoring expression profiles of *Arabidopsis thaliana* gene expression during rehydration process after dehydration using ca. 7000 full-length cDNA microarray. *Plant J.* 34: 868–887.

Partridge, M. and Murphy, D.J. (2009) Role of membrane-bound caleosin and putative peroxygenase in biotic and abiotic stresses responses in Arabidopsis. *Plant Physiol. Biochem.* 47: 796–806.

Perruc, E., Charpenteau, M., Ramirez, B.C., Jauneau, A., Galaud, J.P., Ranjeva, R., et al. (2004) A novel calmodulin-binding protein functions as a negative regulator of osmotic stress tolerance in *Arabidopsis thaliana* seedlings. *Plant J.* 38: 410–420.

Poxleitner, M., Rogers, S.W., Samuels, A.L., Browse, J. and Rogers, J.C. (2006) A role for caleosin in the degradation of oil-body storage lipid during seed germination. *Plant J.* 47: 917–933.

Schauer, S.E., Schlüter, P.M., Baskar, R., Gheyselinck, J., Bolanos, A., Curtis, M.D., et al. (2009) Intronic regulatory elements determine the divergent expression patterns of AGAMOUS-LIKE6 subfamilly members in Arabidopsis. *Plant J.* 59: 987–1000.

Schimdt, M.A. and Herman, E.M. (2008) Suppression of soybean oleosin produces micro-oil-bodies that aggregate into oil-body/ER complexes. *Mol. Plant* 1: 910–924.

Schroeder, J.I., Kwak, J.M. and Allen, G.J. (2001) Guard cell abscisic acid signalling and engeneering drought hardiness in plants. *Nature* 410: 327–330.

Seki, M., Narusaka, M., Abe, H., Kasuga, M., Yamaguchi-Shinozaki, K., Carninci, P., et al. (2001) Monitoring the expression pattern of 1300 Arabidopsis genes under drought and cold stresses by using a full length cDNA microarray. *Plant Cell* 13: 61–72.

Sharabi-Swager, M., Lers, A., Samach, A., Guy, C.L. and Porat R. (2010) Over-expression of the *CBF2* transcriptional activator in Arabidopsis delays leaf senescence and extends plant longevity. *J. Exp. Bot.* 61: 261–273.

Takahashi, S., Katagiri, T., Yamaguchi-Shinozaki, K. and Shinozaki, K. (2000) An Arabidopsis gene encoding a Ca^{2+} binding protein is induced by ABA during dehydration. *Plant Cell Physiol.* 41: 898–903.

Testerink, C. and Munnik, T. (2005) Phosphatidic acid: a multifunctional stress signalling lipid in plants. *Trends Plant Sci.* 10: 1360–1385.

Tisné, S., Reymond, M., Vile, D., Fabre, J., Dauzat, M., Koornneef, M., et al. (2008) Combined genetic and modelling approaches reveal that epidermal cell area and number in leaves are controlled by leaf and plant developmental processes in Arabidopsis. *Plant Physiol.* 148: 1117–1127.

Wang, X. (2004) Lipid signaling. *Curr. Opin. Plant Biol.* 7: 329–336.

Westgate, M.S. and Boyer, J.S. (1985) Osmotic adjustment and the inhibition of leaf, root, stem and silk growth at low water potentials in maize. *Planta* 164: 540–549.